Investigation of Control and Applications of Modular Multilevel Converter with Sub-modular Series IGBTs

Lu Yue
Electrical Engineering Department
University at Buffalo
Buffalo, NY, 14260
Email: luyue@buffalo.edu

Xiu Yao
Electrical Engineering Department
University at Buffalo
Buffalo, NY, 14260
Email: xiuyao@buffalo.edu

***Abstract*—Modular Multilevel Converter (MMC) has been an attractive option for power transmission and has been studied and used for HVDC applications. However, it still has limitations when the number of Sub-Modules per arm is large. To avoid the limitations and exploit the advantages, a method is proposed in this paper which integrates an MMC with series-connected IGBTs in each Sub-Module (SM). The proposed MMC is able to withstand a higher voltage with devices of lower voltage ratings. The series-connected IGBTs are self-balancing. Simulink and real-time simulations both show that, with the proposed method, series IGBTs are able to share a much higher MMC sub-module voltage and recover from voltage imbalances in a timely manner. The proposed series IGBT balancing method causes considerably less loss compared to RCD snubber circuit-based balancing methods.**

I. Introduction

With the development in Flexible AC Transmission, High-Voltage DC Transmission as well as high-power semiconductor devices, the penetration of power electronics technologies is ever increasing. To accommodate high voltage applications, there are generally two solutions. The first one is to connect numerous IGBTs in series. To realize this, press-pack IGBTs were introduced in the 1990s and it has been shown that it is possible to use series-connected IGBTs to transmit HVDC up to 320 KV [1]. Investigations into the use of series-connected IGBTs suggest that the method requires the IGBTs to have matched parameters, precise synchronizations and a similar working environment, etc., otherwise unbalanced switching behavior will occur [2]. Various solutions to above issues have been proposed. One common approach is by adding an RCD snubber circuit in parallel with each IGBT [3]–[5]. However, one drawback is the high energy loss caused by the added resistance. For HVDC applications, where the loss will increase quadratically with voltage, it may become impractical. Another approach is to use active gate control which is able to balance both dynamic and steady-state voltages [6], [7]. However, the active gate control method requires digital controllers making it complicated and expensive to implement.

Table I. Circuit Parameters

Parameter	Value	Parameter	Value
V_{dc}	16 kV	C_{sm}	50 mF
L_p/L_n	1 mH	C_{shunt}	2 uF
R_{load}	60 Ohm	V_{csm}	4 kV
L_{load}	50 mH	V_{cshunt}	1 kV
F_{cr}	1 kHz	$Mod.Method$	N+1 PSPWM
R_{stray}	0.1 Ohm	L_{stray}	1 uH

The second solution is to use multilevel converters [8], [9]. For HVDC applications, Modular Multilevel Converters (MMCs) have become a very popular choice among others [10], [11]. An MMC can be built in various topologies depending on the usage. Researches and studies have been done on different aspects of MMCs including topology improvement [12], voltage balancing control [13], [14], circulating current suppression [15], [16], and the concept of using MMCs as non-sinusoidal current sources for nuclear fusion power [17]. Despite its well-recognized scalability, it is not practical for an MMC to reach any voltage level. To use MMCs on HVDC, there has to be a large number of Sub-Modules per arm and the control of such MMCs will become complex, and thus impractical.

In this paper, a method that combines the use of MMC with series-connected IGBTs to take advantage of both solutions is proposed. The proposed MMC is able to support an output voltage many times the rating of a single IGBT within each Sub-Module. At the same time, it will have the advantages of a regular MMC, such as ease of control, scalability and high reliability. The control of the series IGBTs is based on the control algorithm proposed in [18], where they are controlled in a self-balancing manner without any complex active gate control or resistors which will cause high energy

978-1-5386-1180-7/18/$31.00 ©2018 IEEE

loss. The paper aims at investigating the control and applications of such MMC topology.

II. Circuit Topology and Controller Design

The proposed Modular Multilevel Converter consists of a single-phase half-bridge converter with centralized DC voltage sources. Each arm has four Sub-Modules (SMs). The schematic diagram is shown in Fig. 1 and its parameters are given in Table I.

A. Modular Multilevel Converter Topology

In Table. I and Fig. 1, C_{sm} is the larger capacitor in each Sub-Module while C_{shunt} is the smaller capacitor connected in shunt with each IGBT on the series string. The purpose of C_{sm} is to provide a stable voltage for each SM and power to the load when discharging. The purpose of C_{shunt} is to balance the voltages from $S_{1,1}$ to $S_{4,1}$ so that the IGBTs can share the 4000 V open circuit voltage. L_p/L_n are the arm inductances used to suppress high frequency components in the arm currents. The proposed MMC uses N+1 Phase-Shifted Pulse Width Modulation (N+1 PS-PWM) because it produces mostly second order circulating currents and less high-frequency components compared to 2N+1 PSPWM.

B. Sub-Modular Circuit Topology

On sub-modular level, the proposed MMC functions similarly to a regular MMC. But instead of having one IGBT per switch, it has a string of IGBTs. See Fig. 1 for detailed SM configuration and string configurations. Additional control must be added to ensure the sharing of the SM capacitor voltage, V_{csm} since there are four series IGBTs on each string. The detailed control method is given in the Controller Design section. The stray resistance and inductance intrinsically exist on the wires and they can help limit transient current spikes, reducing the size and rating of the shunt capacitors.

C. Sub-modular Voltage Balancing Controller Design

The controller diagram is shown in Fig. 2. The outer current loop is used to determine controller action, ie., the number of SMs to turn on or off the next cycle. Once the decision is made, the signal is fed to the Voltage Balancing Control (VBC) to determine which SMs will turn on or off based on the feedback C_{sm} voltages and arm currents.

Unlike regular MMCs, the modulations take place inside each Sub-Module. Once a SM receives the signals from the Voltage Balancing Control, the third loop will be initiated, the V_{cshunt} Balancing Control Loop. Fig. 3 provides an illustration on the V_{cshunt} balancing process. The feedback capacitor voltages $V_{cshunt1}$ and $V_{cshunt2}$ are used to bias the triangular carrier signal assigned to the sub-module to generate a new dedicated carrier for each IGBT in series. The new carriers are then compared

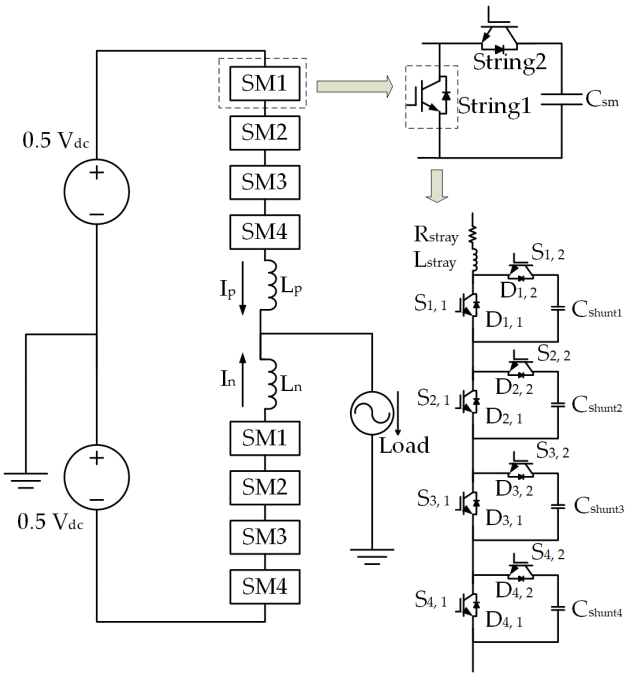

Figure 1. The topology of the MMC combined with series IGBTs.

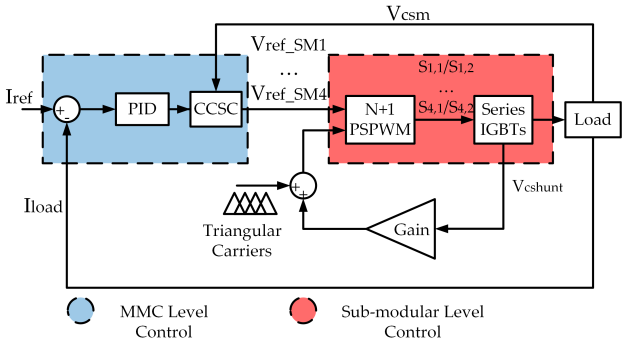

Figure 2. The overall controller diagram.

with a shared reference to generate gate signals. Since $V_{cshunt1}$ is higher than $V_{cshunt2}$, the switch $S_{1,1}$ will stay on longer than $S_{2,1}$ as depicted in Fig. 3. This will ensure that C_{shunt1} gets inserted to the circuit shorter than C_{shunt2}. In other words, C_{shunt1} will get charged less and discharged more than C_{shunt2}. Therefore, the two capacitors will eventually have the same voltages. By adjusting k_1 and k_2, one can control the voltage balancing speed. An example of this mechanism in operation is given in Fig. 4. $V_{cshunt1}$ is lower than $V_{cshunt2}$. As a result, the controller creates delays which ensure that C_{shunt1} gets charged more and discharged less than C_{shunt2}. In this way, $V_{cshunt1}$ will rise while $V_{cshunt2}$ falls and eventually they will converge. It can also be seen in Fig. 4 that as the voltage difference diminishes, so does the delay and when the voltages become equal, the delay will become zero. The control method can be expanded to more than two series IGBTs.

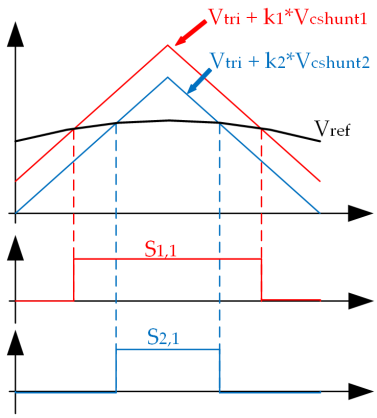

Figure 3. Illustration of the delay generation process.

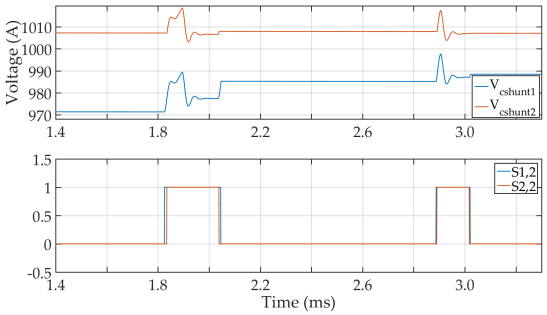

Figure 4. V_{cshunt} and gate signals relationship.

D. Circulating Current Suppression Controller Design

Since the proposed circuit is an MMC on the system level, it requires a circulating current suppression controller (CCSC). Studies have shown that the arm currents in an MMC contains mainly three components: DC component, AC component, and circulating current which is dominantly 2nd order harmonics. [19]. Circulating current will increase loss as well as cause devices to have higher voltage and current ratings.

In this paper, circulating current suppression is achieved by using non-ideal Proportional Resonant (PR) controllers [20]. The transfer function of one non-ideal PR controller is given in Eq. 1:

$$G_{pr}(s) = k_p + \frac{2k_r\omega_c s}{s^2 + 2\omega_c s + \omega_0^2} \tag{1}$$

where k_p and k_r are proportional gain and resonant gain, ω_c is the cutoff frequency; ω_0 is the resonant frequency.

With a non-ideal PR controller, one can extract harmonics of a certain frequency determined by ω_0 and use it to generate adjustments to the reference signals for each arm. Multiple PR controllers can be used in parallel to eliminate higher order components in circulating current. Given that the fundamental frequency is 60 Hz, three non-ideal PR controllers are used for harmonics of 120 Hz, 240 Hz and 360 Hz respectively. The schematic of CCSC is shown in Fig. 5.

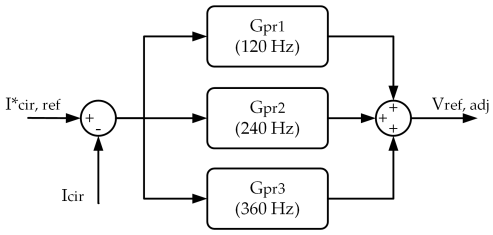

Figure 5. The schematic of the circulating current suppression controller

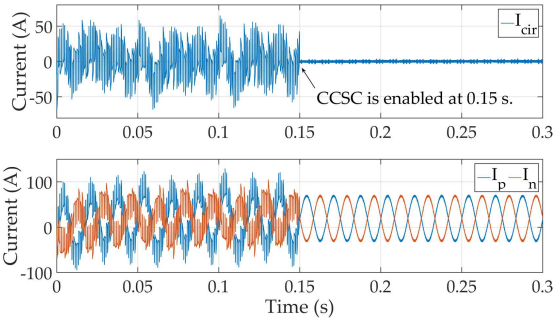

Figure 6. Circulating current and arm current waveforms before and after CCSC is enabled.

The output of the CCSC, $V_{ref,adj}$, is sent to adjust the reference signals to eliminate circulating current based on the following equations.

$$V_{p,ref} = V_{dc} - V_{ref0} - V_{ref,adj} \tag{2a}$$

$$V_{n,ref} = V_{ref0} - V_{ref,adj} \tag{2b}$$

where $V_{p,ref}$ and $V_{n,ref}$ are the adjusted references for the upper and lower arms, respectively; V_{ref0} is the output of the PI controller, or the unadjusted reference.

Fig. 6 shows the circulating current and arm currents before and after the CCSC is enabled. From the figure, it can be seen that the circulating current is reduced and the resulting arm currents mostly contain two components: the DC component and the AC component.

E. Device Ratings and Counts

In this paper, main devices are defined as $S_{j,1}$, and $D_{j,1}$. Auxiliary devices refer to $S_{j,2}$, $D_{j,2}$ and C_{shuntj} (j = 1…4). After the main string turns off, due to the

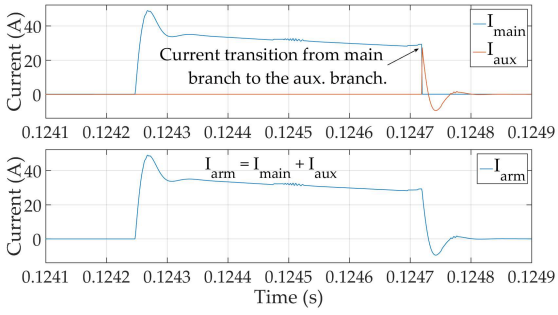

Figure 7. Main, auxiliary and arm current waveforms.

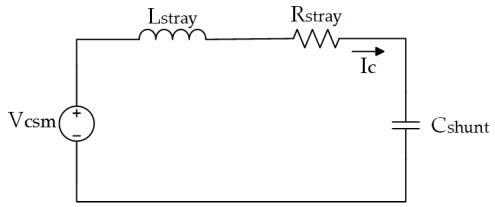

Figure 8. Equivalent circuit of a main branch during turn-off.

stray elements, the current will remain near the steady-state level. Therefore, it must flow through the shunt branch and charge C_{shunt} as shown in Fig. 7. As a result, the main devices should have the same current rating as one regular MMC switch but one Nth the voltage rating. Auxiliary devices, on the other hand, only need to withstand a surge current equal to the arm current and thus are even lower in ratings. The low current rating auxiliary devices cause less energy loss compared to shunt resistors in RCD snubber circuits.

Fig. 8 shows the equivalent circuit of a main branch during turn-off. V_{csm} represents the sub-module capacitor voltage which can be seen as constant because the turn-off process is much shorter compared to C_{sm} time constant. L_{stray} and R_{stray} are the total stray elements inside a sub-module. C_{shunt} is the total shunt capacitance of a series branch. From Fig. 8, one can see that the turn-off process is equivalent to charging C_{shunt} through the RLC branch with $I_c(t)$ whose initial value is the arm current before turn-off.

Given the above definitions, to evaluate the voltage ratings of C_{shunt} and switching devices, the worst case must be considered where the charging current is at the highest while the shunt capacitance is at the lowest. The highest charging current I_c appears when the main branch switches off at the peak of upper arm current. Upper arm current can be calculated with the following equation:

$$V_{dc} * i_{arm}(t) = v_{load}(t) * i_{load}(t) \tag{3}$$

Rearranging the above equation, one can get the expression for $i_{arm}(t)$ as shown below.

$$i_{arm}(t) = \frac{1}{V_{dc}}[\frac{V_m I_m}{2} cos(\theta) - \frac{V_m I_m}{2} cos(2\omega t + \theta)] \tag{4}$$

where V_m, I_m, ω and θ are load voltage amplitude, load current amplitude, fundamental angular frequency and load voltage-current phase angle. The first and second terms correspond to the DC and AC components, respectively. Therefore, the highest arm current occurs at the peak of the AC component. On the other hand, the lowest shunt capacitance appears when V_{cshunt} are

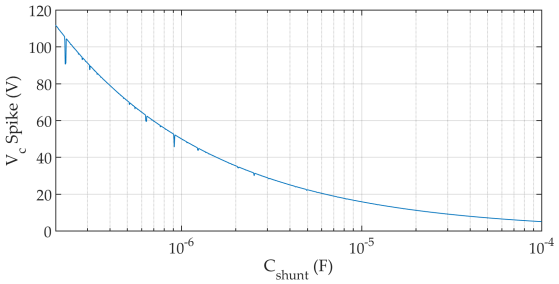

Figure 9. The relationship between v_c spike and C_{shunt}

balanced, ie., when all C_{shunt} get inserted at the same time.

Given the conditions, one can write the following equations:

$$V_{csm} = L_s C_s \frac{d^2 v_c}{dt^2} + R_s C_s \frac{dv_c}{dt} + v_c \tag{5a}$$

$$v_c(0) = 0 \tag{5b}$$

$$\frac{dv_c}{dt} |_{t=0} = I_{arm,peak} \tag{5c}$$

where L_s, R_s and C_s are short for L_{stray}, R_{stray} and C_{shunt}, v_c is the voltage rise across C_{shunt} caused by I_c. Solving Eq. 5, one can get the expression for v_c in terms of C_s. Fig. 9 shows the relationship between v_c and C_s. It can be concluded that lower C_{shunt} can reduce the size and cost but increase the voltage stress on switching devices, or vice versa.

To reduce device voltage ratings by a factor of N, 2N main devices and 2N auxiliary devices are needed per SM. The proposed voltage balancing controller does not require local digital processing: opamp-based analog circuits will suffice, which is an advantage compared to active gate control and its related methods.

III. Simulation Results and Analysis

A. Matlab/Simulink Simulation Results

The Matlab/Simulink simulation results of the MMC's load supplying and reference tracking abilities are demonstrated in Fig. 10. As can be seen from the figure, the MMC is able to track the 60 Hz sinusoidal reference closely with an amplitude of 100 A. The output voltage is 4000 V per level as determined by the modulation method. Fig. 11 demonstrates the effect of the shunt capacitor voltage balancing controllers. The initial voltages of each series IGBT differ from each other. At the beginning of the simulation, the controllers turn on and one can see that the voltages are regulated in around 0.01 s. Also, during the transient period, no high voltage spikes appear even though there are delays in the gate signals, indicating that the devices are safe during that dynamic period.

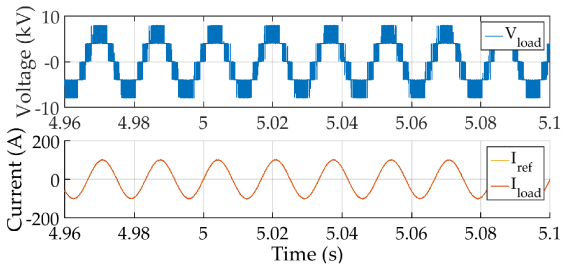

Figure 10. MMC output waveforms from Simulink simulation.

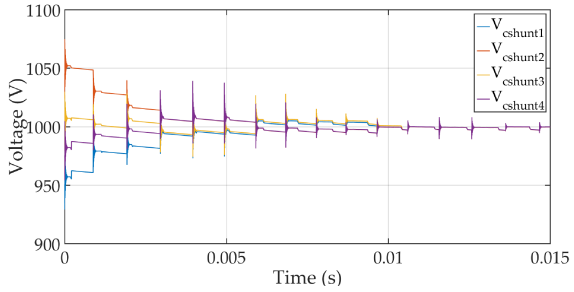

Figure 11. Voltage balancing of the Simulink model.

B. Real-time Simulation Results

To further verify the circuit operation, real-time simulations were conducted on an OP4510 platform. The simulations run at 50 μs calculation step intervals as pre-determined by the platform. During the real-time simulation, the V_{cshunt} imbalances are kept until 0.5 second into the oscilloscope image capture. The real-time simulation results are shown in Fig. 12 and 13, captured with a Tektronix DPO4045B oscilloscope. It can be seen that the MMC is able to output clean multilevel voltages and sinusoidal current and the voltage balancing among $V_{cshunts}$ recovered in a timely manner.

Fig. 14 demonstrates the real-time simulation results of the circulating current suppression controller. After it is enabled, the CCSC is able to suppress the circulating current and there are mainly DC and AC components in the arm currents.

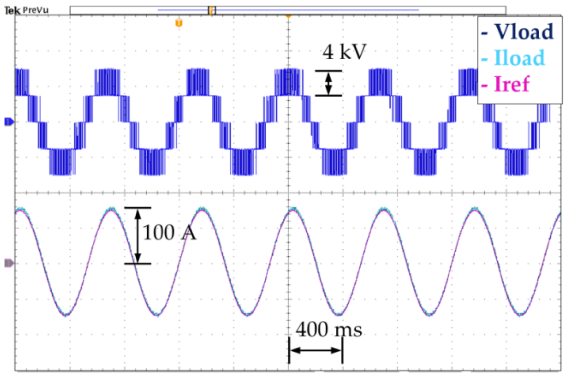

Figure 12. MMC output waveforms in real-time simulation.

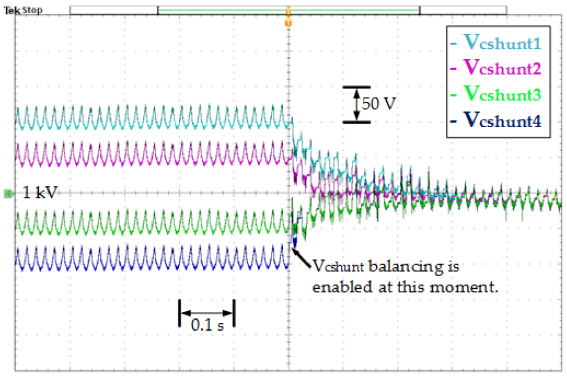

Figure 13. V_{cshunt} before and after balancing control initiates.

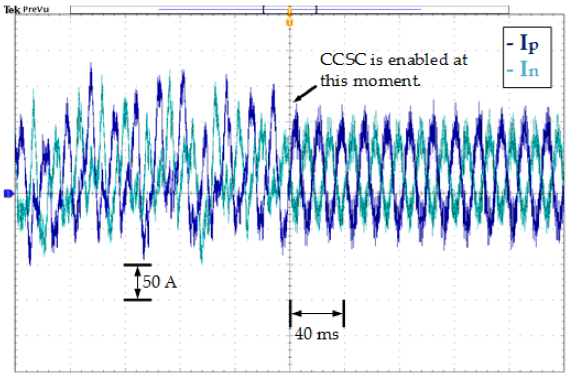

Figure 14. Arm currents before and after CCSC is enabled.

C. Loss Comparison with RCD Snubber Circuit Method

To evaluate the power loss of the auxiliary branch, commercial IGBT/diode FGA25S125P from Fairchild is chosen as the auxiliary switches. FGA25S125P is rated at 1250 V, 25 A and capable of handling 75 A pulse currents. By consulting the datasheet, it can be determined that the energy loss of one switch is around 3 mJ per cycle.

As mentioned in the Introduction, one way to balance the voltages among series IGBTs is through the use of RCD snubber circuits. Fig. 15 provides the schematic of one IGBT with RCD snubber circuit. The main advantages of the RCD method are its simplicity, low cost and fast response. However, due to the use of resistors, the RCD method is prone to higher losses.

Reference [3] provides the equations to calculate R_s, C_s and R_b. Using the equations, the RCD circuit parameters for the same series IGBTs can be determined: $C_s = 1\ \mu F$, $R_s = 180\ \Omega$, $R_b = 65\ k\Omega$. The energy loss

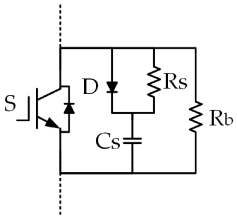

Figure 15. One IGBT with RCD snubber circuit.

over R_b alone can be determined:

$$p_{rb} = V_{IGBT}^2 / R_b = (1000\ V)^2 / 65000\ \Omega = 15.4\ W \quad (6)$$

where V_{IGBT} is the desired voltage of one IGBT/diode in the series group. Note that this power loss only occurs when the main IGBT is off, which is half of the switching cycle on average. Therefore, the energy loss on R_b per cycle can be calculated with Eq. 7:

$$E_{rb} = p_{rb} * T_{off,avg} = 15.4\ W * 0.5\ ms = 7.7\ mJ \quad (7)$$

R_b alone has over twice the energy loss of an auxiliary switch. On the other hand, R_s-C_s branch functions similarly to the proposed $S2, j$-$C_{shunt,j}$ circuit, both causing less power loss compared to R_b. Therefore, the proposed circuit topology has a lower energy loss compared to RCD snubber method.

IV. Conclusions

An MMC combined with sub-modular series IGBTs is proposed in this paper. The MMC is able to withstand a much higher voltage with devices rated at a fraction of that voltage rating. The MMC is also equipped with a non-ideal Proportional Resonant controller-based circulating current suppression controller that eliminates the unwanted components from arm currents. To control the series IGBT strings, a control method is implemented which relies on creating time delays to the IGBTs' turn-on/off signals to maintain voltage balance. Simulation results show that the proposed MMC is able to supply a load, and the self-balancing control is able to regulate imbalance shunt capacitor voltages in a short time. An auxiliary device selection guide is also included showing the trade-off between lower device ratings and lower voltage spikes. Finally, a loss comparison is also presented demonstrating that the proposed circuit consumes less energy compared with the RCD snubber circuit.

Acknowledgment

This material is based upon work supported by the National Science Foundation under grant no. ECCS 1711659.

References

[1] B. Jacobson, Y. Jiang-Häfner, P. Rey, G. Asplund, M. Jeroense, A. Gustafsson, and M. Bergkvist, "Hvdc with voltage source converters and extruded cables for up to +/-300 kv and 1000 mw," 2006.

[2] J. Baek, D. Yoo, and H. Kim, "High-voltage switch using seriesconnected igbts with simple auxiliary circuit," *IEEE Transactions on Industry Applications*, vol. 37, no. 6, pp. 1832 – 1839, 2001.

[3] J. Chen, J. Lin, and T. Ai, "The techniques of the serial and paralleled igbts," in *1996 IEEE 22nd International Conference on Industrial Electronics, Control, and Instrumentation*, Aug. 1996, pp. 999–1004.

[4] D. Ning, X. Tong, M. Shen, and W. Xia, "The experiments of voltage balancing methods in igbts series connection," in *2010 Asia-Pacific Power and Energy Engineering Conference (APPEEC)*, Apr. 2010, p. 1–4.

[5] B. Wang, T. Zheng, and J. Zhang, "Voltage controlled variable capacitor based snubber for the further reduction of igbt's turn-off loss," in *2014 IEEE Energy Conversion Congress and Exposition (ECCE)*, Nov. 2014, pp. 935–940.

[6] I. Baraia, J. A. Barrena, G. Abad, J. Segade, and U. Iraola, "An experimentally verified active gate control method for the series connection of igbt/diodes," *IEEE Transactions on Power Electronics*, vol. 27, no. 2, pp. 1025–1038, 2012.

[7] Y. Lobsiger and J. W. Kolar, "Closed-loop di/dt and dv/dt igbt gate driver," *IEEE Transactions on Power Electronics*, vol. 30, no. 6, pp. 3402–3417, 2015.

[8] L. Franquelo, J. Rodriguez, J. Leon, S. Kouro, R. Portillo, and M. Prats, "The age of multilevel converters arrives," *IEEE Industrial Electronics Magazine*, vol. 2, no. 2, pp. 25 – 39, 2008.

[9] R. Marquardt, "Stromrichterschaltungen mit verteilten energiespeichern," German Patent, 2001.

[10] S. Fazel, S. Bernet, D. Krug, and K. Jalili, "Design and comparison of 4-kv neutral-point-clamped, flying-capacitor, and series-connected h-bridge multilevel converters," *IEEE Transactions on Industry Applications*, vol. 43, no. 4, pp. 1032 – 1040, 2007.

[11] P. Cortes, A. Wilson, S. Kouro, J. Rodriguez, and H. Abu-Rub, ""model predictive control of multilevel cascaded h-bridge inverters," *IEEE Transactions on Industrial Electronics*, vol. 57, no. 8, pp. 2691 – 2699, 2010.

[12] G. Son, H. Lee, T. Nam, Y. Chung, U. Lee, S. Baek, K. Hur, and J. Park, "Design and control of a modular multilevel hvdc converter with redundant power modules for noninterruptible energy transfer," *IEEE Transactions on Power Delivery*, vol. 27, no. 3, pp. 1611–1619, 2012.

[13] M. Glinka and R. Marquardt, "A new ac/ac multilevel converter family," *IEEE Transactions on Industrial Electronics*, vol. 52, no. 3, pp. 662 – 669, June, 2005.

[14] S. Rohner, S. Bernet, M. Hiller, and R. Sommer, "Modulation, losses, and semiconductor requirements of modular multilevel converters," *IEEE Transactions on Industrial Electronics*, vol. 57, no. 8, pp. 2633 – 2642, 2010.

[15] W. Do, S. Kim, T. Kim, and R. Kim, "A study of circulating current in mmc based hvdc system under an unbalanced grid condition," *Transactions of the Korean Institute of Electrical Engineers*, vol. 64, no. 8, pp. 1193 – 1201, 2015.

[16] J. Moon, J. Kim, Cand Park, D. Kang, and J. Kim, "Circulating current control in mmc under the unbalanced voltage," *IEEE Transactions on Power Delivery*, vol. 28, no. 3, pp. 1952 – 1959, 2013.

[17] X. Yao, Y. Huang, F. Guo, and J. Wang, "Advanced concepts for vertical stability power supply in fusion devices," *IEEE Transactions on Plasma Sciences*, vol. 40, no. 3, pp. 761 – 768, 2012.

[18] L. Yang, P. Fu, X. Yao, and J. Wang, "A module based self-balanced series connection for igbt," in *2014 IEEE Energy Conversion Congress and Exposition (ECCE)*, 2014.

[19] S. Rohner, S. Bernet, M. Hiller, and R. Sommer, "Analysis and simulation of a 6 kv, 6 mva modular multilevel converter," in *Industrial Electronics, 2009. IECON '09. 35th Annual Conference of IEEE*, Feb. 2009.

[20] S. Li, X. Wang, Z. Yao, and Z. Li, T Peng, "Circulating current suppressing strategy for mmc-hvdc based on nonideal proportional resonant controllers under unbalanced grid conditions," *IEEE Transactions on Power Electronics*, vol. 30, no. 1, pp. 387 – 397, 2015.